

Article

# Optimization, by Means of a Design of Experiments, of Heat Processes to Increase the Erosive Wear Resistance of White Hypoeutectic Cast Irons Alloyed with Cr and Mo

Alejandro Gonzalez-Pociño, Florentino Alvarez-Antolin \*  and Juan Asensio-Lozano 

Materials Pro Group, Departamento de Ciencia de los Materiales e Ingeniería Metalúrgica, Universidad de Oviedo, Independencia 13, 33004 Oviedo, Spain; UO204622@uniovi.es (A.G.-P.); jasensio@uniovi.es (J.A.-L.)

\* Correspondence: alvarezflorentino@uniovi.es; Tel.: +34-985-181-949

Received: 28 February 2019; Accepted: 29 March 2019; Published: 2 April 2019



**Abstract:** To identify the design parameters in heat treatments that have a significant effect on the erosive wear resistance of hypoeutectic high chromium white cast irons, a design of experiment was applied to a white cast iron with 18wt.% Cr and 2wt.% Mo. The analyzed factors were the destabilization heat treatment of austenite (1000 or 1100 °C, for 4 or 8 h), different quench cooling media (in air or oil), different tempering treatments (200 or 500 °C, for 3 or 6 h), and the application of an ionic nitriding treatment. Despite what was expected, the nitriding treatment was not found to have a significant effect on said wear resistance. However, it is concluded that the highest wear resistance is obtained with the shortest dwell time at the destabilization temperature (4 h), quenching in oil, and with the shortest tempering times (3 h). Among the nitrated samples, the highest nitrated layer thicknesses were obtained when the destabilization temperature of the austenite was 1000 °C and the tempering temperature was 200 °C.

**Keywords:** high chromium white cast iron; destabilization of the austenite; erosive wear; plasma nitriding

## 1. Introduction

White cast irons with a percentage of Cr greater than 15wt.% show two microstructural peculiarities that condition their properties. One of these is that the matrix phase of the eutectic constituent is, in fact, unstable austenite at room temperature (retained austenite), which affords a greater toughness compared to other white cast irons and also allows them to be machined when subjected to an isothermal treatment that transforms the austenite into pearlite [1]. The other peculiarity is that the carbides that form part of their eutectic are mixed  $M_7C_3$  carbides, typically  $(Fe,Cr)_7C_3$ , which have a hardness value between 1200 and 1600 HV [2]. The content of  $M_7C_3$  type eutectic carbides increases gradually with the increase in chromium content [3]. These carbides have a similar morphology to bars or plates [4]. These cast irons are widely used in applications that require a high resistance to wear, as would be the case of processes linked to the treatment of raw materials in the cement industry and thermal power stations, as well as in crushing and grinding processes in the mining industry. Abrasion resistance of white cast irons depends greatly on the properties and microstructure of the material, as well as on the wear conditions [5]. Martensite may form at relatively low cooling rates due to the high hardenability conferred by a high alloy content in solid solution of austenite prior to quenching. One such alloying element is chromium, which allows martensite to form by air cooling [1]. However, wear resistance is improved if the precipitation of chromium-rich secondary carbides [6,7], uniformly distributed in a predominantly martensitic matrix, is promoted and if the

percentage of retained austenite is reduced [8]. These secondary carbides are precipitated as a result of the destabilization of austenite at temperatures around 1000 °C or higher [4,7,9–19]. This precipitation favors an increase in the  $M_s$  temperature, reducing the risk of cracking in cooling media with harsher cooling conditions than air [1]. Quenching in oil would decrease the percentage of retained austenite at room temperature as compared to air quench, as in the former a higher cooling rate between  $M_s$  and  $M_f$  will take place. Hence, a higher conversion of austenite into martensite. Tempering temperatures according to industrial practices usually fall within the 200–250 °C range [1]. At higher temperatures of between 400 and 600 °C, however, it should be possible to achieve a second destabilization of the retained austenite, leading to its transformation into new martensite [20]. Higher hardness values would be obtained with double tempering around 500 °C [21]. The addition of Mo produces a drop in both the liquidus temperature and the eutectic temperature. This in turn leads to an increase in the size of the eutectic cell and greater spacing between the carbide particles [22]. The addition of Mo likewise increases the hardenability of the material [23], increasing its hardness [24] and wear resistance [25–27]. Furthermore, the presence of Mo leads to the formation of  $M_2C$  carbides, and it has been found that these nucleate from  $M_7C_3$  carbides to spread through the martensitic matrix [10,28]. This precipitation may occur during high temperature tempering [14]. In steels, a thermochemical nitriding treatment produces surface hardening via the formation of subnitrides of Cr, V, Mo, and Al in the tempered martensite matrix [29,30]. However, there are no previous reports of the nitriding of high chromium white cast irons. In the case of steels belonging to the Fe–Cr–Mo system, the type of  $(CrMo)_xN_y$  nitrides will depend on the Cr/Mo ratio [30].

The aim of this paper is to analyze the influence of the process variables related to the quenching, tempering and possible subsequent nitriding of a white cast iron with 18 wt.% Cr and 2 wt.% Mo on its hardness and resistance to erosive wear. The temperatures chosen in this study to determine the possible effect of temperature on the destabilization of austenite were 1000 and 1100 °C, the goal being to determine whether an increase of this temperature up to 1100 °C might lead to an improvement in wear resistance due to an increase in the precipitation of these secondary carbides.

## 2. Materials and Methods

The experimental method applied was a design of experiments (DOE) with 6 factors, 2 levels for each factor, and 8 experiments in all [31]. The purpose of applying the DOE statistical technique is to modify normal working conditions deliberately so as to produce changes in some of the responses under study. These deliberate changes in normal working conditions are carried out on specific, previously-selected factors of the manufacturing process. Full factorial designs of experiments require a large number of experiments, which grow exponentially depending on the number of factors studied. When there are  $k$  factors to study in a full factorial DOE, the number of tests is  $2^k$ , where 2 is the number of levels applied to each of the factors. Fractional DOEs allow a large number of factors to be studied by means of a much smaller number of experiments, assuming the loss of information of possible interactions between factors, which are not usually very significant in practice. It should be noted that fractional factorial DOEs are symbolized as  $2^{k-p}$ , where 2 is the number of levels,  $k$  the number of factors and  $p$  the degree of fractionation. In our case, the design of experiments employed would be  $2^{6-3} = 8$ . Table 1 shows the chemical composition of the white cast iron under analysis. Table 2 shows the analyzed factors and levels, while Table 3 displays the array of experiments, together with the confounding pattern. The analyzed factors correspond to the process variables related to quenching, tempering and possible subsequent nitriding. The set of generators associated with this array of experiments is  $D=AB$ ,  $E=AC$  and  $F=BC$ , of which the resulting relation definition is  $I=ABD=ACD=BCF$ , where  $I$  is a column formed only by some (+1) [31]. This means that the interactions  $ABD$ ,  $ACD$ , and  $BCF$  are confounded with the mean. The resolution of this design is III; i.e., the main effects are confounded with the interactions of two factors [31]. In general, a DOE with resolution  $N$  is one in which no effect of  $q$  factors is confounded with another containing less than  $N-q$  factors. In our case, the proposed DOE is of type  $2^{k-p}$ , which means that it has a resolution of III because the main

effects are confounded with the interactions of 2 factors. Note that 3 (resolution) = 1 (main effects) + 2 (interactions of 2 factors). The “Confounding Pattern” column in Table 3 indicates those interactions of two factors which are confounded with the main effects.

**Table 1.** Chemical composition (% in weight).

C	Si	Mn	Cr	Mo	Fe
3.02	1.17	0.80	18.21	2.05	≤74.75.

**Table 2.** Factors and levels analyzed in the design of experiments (DOE) (cooling medium after tempering: Air).

Code	Factors	Levels	
	Metallurgical Parameter	Level -1	Level +1
A	Destabilization temperature of austenite (°C)	1000	1100
B	Dwell time at the destabilization temperature (h)	4	8
C	Nitriding	No	Yes
D	Quench cooling medium	air	oil
E	Tempering temperature (°C)	200	500
F	Dwell time at temperature during tempering (h)	3	6

**Table 3.** Array of Experiments.

No	A	B	C	D	E	F	Confounding Pattern
1	-1	-1	-1	+1	+1	+1	
2	+1	-1	-1	-1	-1	+1	A+BD+CE
3	-1	+1	-1	-1	+1	-1	B+AD+CF
4	+1	+1	-1	+1	-1	-1	C+AE+BF
5	-1	-1	+1	+1	-1	-1	D+AB+EF
6	+1	-1	+1	-1	+1	-1	E+AC+DF
7	-1	+1	+1	-1	-1	+1	F+BC+DE
8	+1	+1	+1	+1	+1	+1	AF+BE+CD

The analyzed responses were:

- The Vickers hardness, representative of each of the 8 experiments. The applied load was 125 kgf (1225.83 N). In all cases, 10 indentations were made in each of the samples. The hardness values were obtained on a cross-section in areas at a distance from the edge of the specimen, avoiding indentations in areas near the edge. Moreover, face milling was used to remove 1 mm of the surface material so as to avoid the influence of any possible surface decarburization.
- The microhardness of the matrix phase, that is to say austenite mainly transformed into martensite, and pre-existing secondary carbides dispersed in the former. These secondary carbides were obtained during destabilization of austenite at 1000 or 1100 °C, which is a former stage prior to cooling in air or oil. This practice of austenite destabilization allows for austenite depletion in carbon and alloying elements in solid solution, which allows  $M_s$  to increase enabling to increase the section size to quench without cracking as well as to obtain less retained austenite after quenching. In the present experimental procedure, the applied load was 0.05 kgf (0.49 N), performing 10 indentations in each of the samples. Similar to the previous case, microhardness measurements were made on the cross-section after removing 1 mm of the material by milling.
- The erosive wear resistance, which was measured by means of compressed air blasting with corundum particles according to the ASTM G76 standard, applying a pressure of 4 bar, a flow rate of 1 g/s and a 30° angle of incidence on the sample surface. Five repetitions were performed in each test. The duration of each trial was 1 minute. The dimensions of the tested specimens were those of a prism measuring 60 mm × 40 mm × 15 mm.

The effect of a factor on the variation in the response function is defined as a consequence of the variation of said factor. The main effect of a factor indicates how much the response changes when this factor changes from its  $-1$  level to its  $+1$  level. The effect of one factor may often depend on the value that another takes. When this occurs, these factors are said to interact. Interactions between 2 factors are defined as the variation between the average effect of one factor with the other factor at its low level,  $-1$ , and the average effect of the same factor with the other at its high level,  $+1$ . The interactions between several factors are similarly defined. The importance of the main effects tends to be greater than the importance of the interactions of 2 factors, while the latter are in turn greater than the interactions of 3 factors, and so on.

The experimental response was subject to random variation. This variation followed a normal law, where its standard deviation reflects experimental error. The effects are linear combinations of the responses. Hence, applying the central limit theorem (CLT), they followed a normal law. Each main effect may be considered a random variable where the obtained value is an estimate of its mean; hence, this value is accompanied by the estimation of its standard deviation. If all the effects were non-significant, they would follow an  $N(0,\sigma)$  law and would thus appear aligned in a representation of the effects on a normal probability plot. If any effect was significant, it will follow an  $N(\mu,\sigma)$  law, not appearing aligned with the non-significant effects. The standardized effect is the ratio between the difference in the value of the response and its mean and standard deviation. This represents not only whether the value of the variable is above or below the mean, but also how far it deviates from it. Those standardized effects that deviate from the straight line towards the ends on the normal probability plot are significant. Those that deviate to the left indicate that the value of the response increases at their  $-1$  level, while, analogously, those that deviate to the right indicate that the value of the response increases at their  $+1$  level [31]. The standardized effects were compared on a normal probability plot using the Statgraphics Plus (version 5.1) program.

The microstructural changes in the eight experiments were analyzed by means of optical microscopy and scanning electron microscopy. Table 4 shows the parameters used in the nitriding process. The optical microscope employed was a NIKON Epiphot 200 (Nikon, Tokyo, Japan) and the scanning electron microscopy employed was a JEOL JSM-5600 (JEOL, Nieuw-Vennep, The Netherlands). The method followed consisted of washing the plasma treatment chamber with mixing gas for a period of 10 min, after which the treatment commenced.

**Table 4.** Parameters used in the plasma nitriding process.

Gas Mixture	70vol.%N <sub>2</sub> + 30vol.%H <sub>2</sub>
Gas flow(cm <sup>3</sup> /s)	0.14
Temperature (°C)	540
Pressure (Pa)	400
Time (min)	120
Output voltage (V)	500

### 3. Results

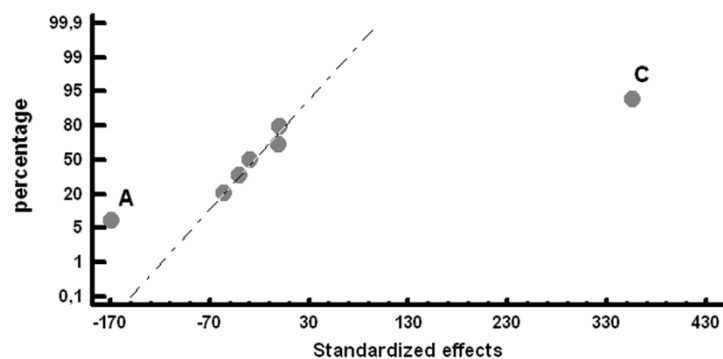
Table 5 shows the mean values obtained for the studied responses and the standardized effects corresponding to the Factors and Interactions indicated in the column denominated “Confounding Pattern”. The row corresponding to the mean shows the average value obtained for each of the responses.

**Table 5.** Mean values and standardized effects for the analyzed parameters.

Experiment	Mean Hardness HV125		Microhardness of Matrix Phase HV0.05		Wear (mg/min)		Confounding Pattern
	Values	Effect	Values	Effect	Values	Effect	
1	833	948.6	764	879.2	59.64	60.73	Mean
2	679	-169.2	603	-186.5	61.9	-0.23	A+BC+CE
3	877	0.2	792	16	61.92	0.70	B+AD+CF
4	693	356.2	643	375.5	59.2	0.13	C+AE+BF
5	1178	-55.2	1129	-36	58.8	-2.55	D+AB+EF
6	1104	-0.2	989	-31.5	61.18	0.00	E+AC+DF
7	1245	-28.7	1205	18	63.04	0.91	F+BC+DE
8	980	-40.2	909	42	60.18	-0.06	AF+BE+CD

Figures 1–3 show the representation of these standardized effects on a normal probabilistic plot, highlighting those that have a significant effect on these responses (these Factors do not appear aligned in a representation of the effects on a normal probability plot).

1. Figure 1 shows that Factors A (austenitization temperature) and C (nitriding) have a significant effect on the representative hardness of the material: If Factor A is placed at its  $-1$  level ( $1000\text{ }^{\circ}\text{C}$ ) and Factor C at its  $+1$  level (nitriding treatment), there is a significant increase in hardness.
2. Figure 2 shows the analysis of the hardness on the matrix constituent, mainly made up of martensite, retained austenite and secondary carbides formed during the destabilization of austenite. It is confirmed that if the aforementioned Factors (destabilization heat temperature of the austenite and nitriding treatment) are placed at their respective  $-1$  and  $+1$  levels, there is an increase in said hardness.
3. Figure 3 shows that the Factors found to have a significant effect on erosive wear are B (dwell time at the destabilization heat temperature of austenite), D (cooling medium used in the quench) and F (tempering time). To increase the wear resistance of the material, these Factors should be placed at their respective  $-1$  (dwell time at the destabilization temperature of austenite: 4 h),  $+1$  (quenching in oil) and  $-1$  (dwell time at the tempering temperature: 3 h) levels. It is worth noting that, in this case, neither the nitriding treatment nor the tempering temperature was found to have a significant effect on said erosive wear resistance.

**Figure 1.** Standardized effects on the overall hardness, on a normal probability plot.

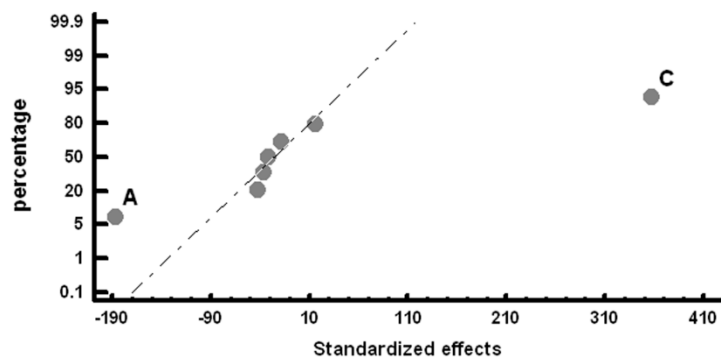


Figure 2. Standardized effects on the hardness of the matrix, on a normal probability plot.

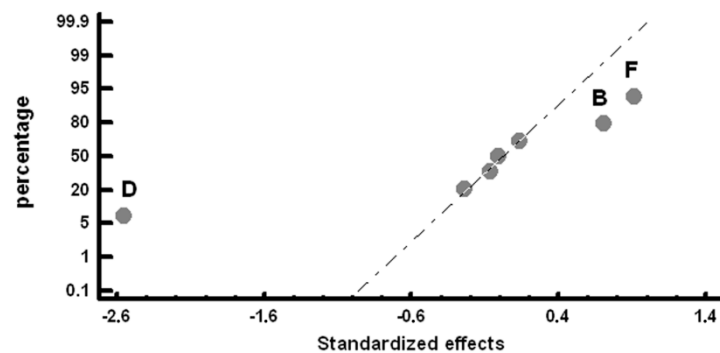
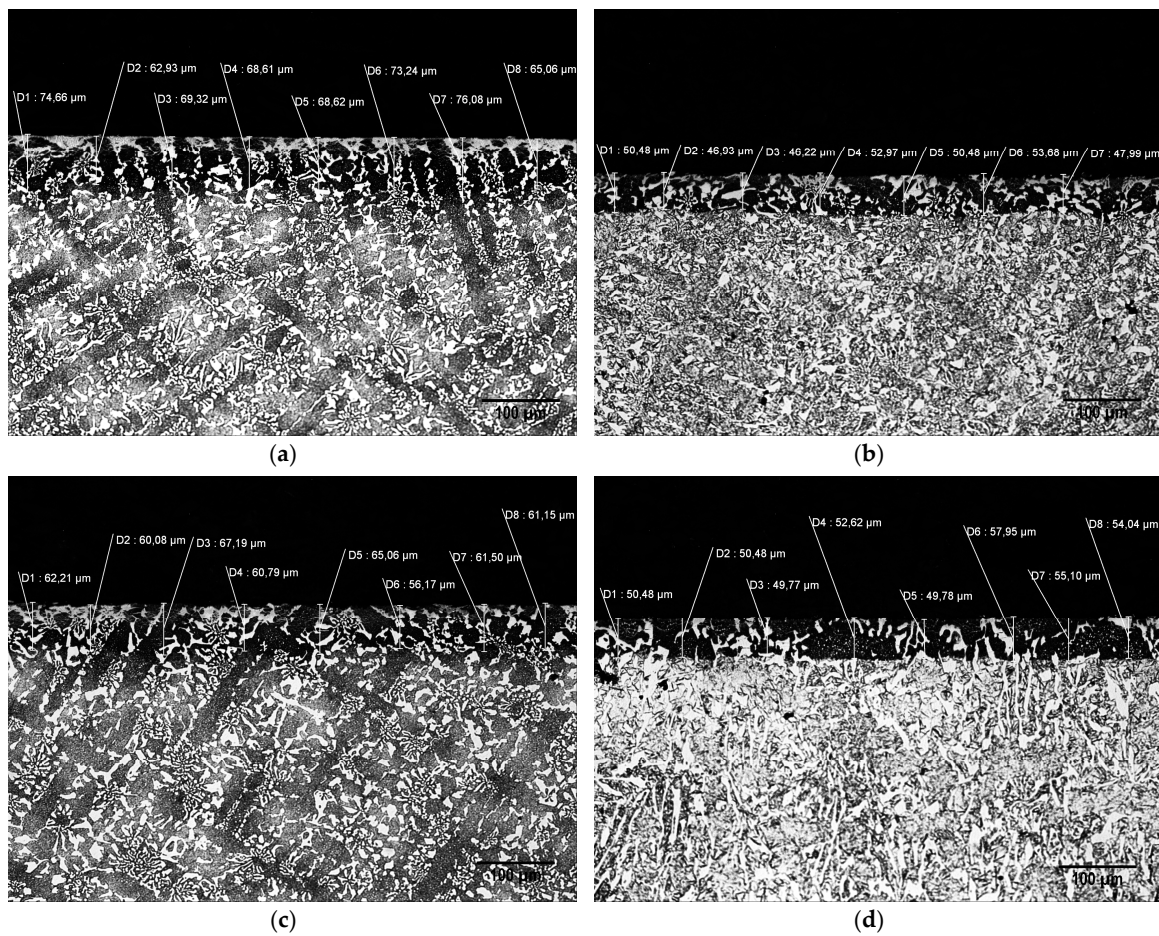
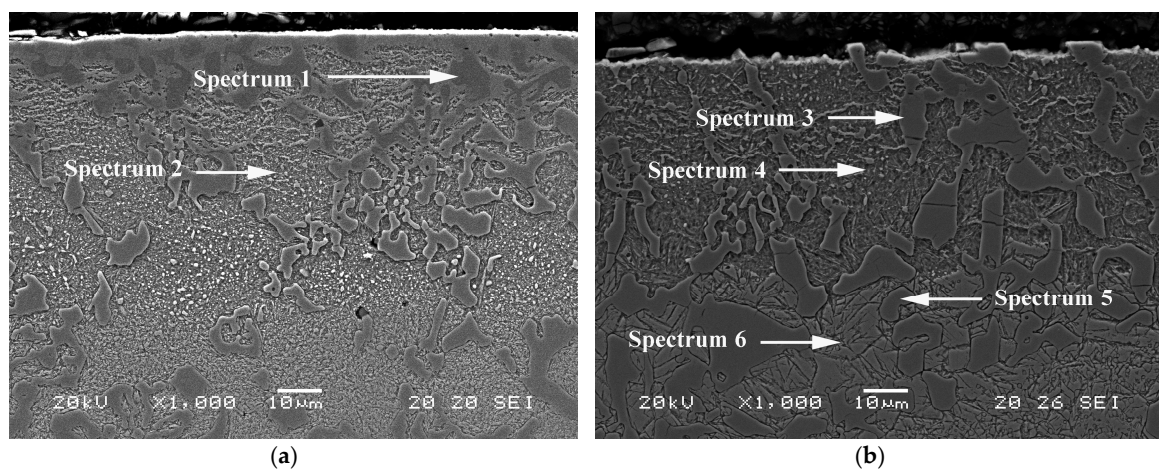


Figure 3. Standardized effects on the erosive wear, on a normal probability plot.

Figure 4 provides a representative image of the thickness of the nitrated layer in Experiments 5 to 8. It can be seen that the thickness of the nitrated layer varies between 50 and 75  $\mu\text{m}$ . The greatest layer thicknesses are obtained in Experiments 5 and 7, where the mean thicknesses are 70 and 62  $\mu\text{m}$ , respectively. These two experiments coincide in terms of the temperature applied to destabilize the austenite (1000  $^{\circ}\text{C}$ ) and the lowest tempering temperature (200  $^{\circ}\text{C}$ ). Figure 5 shows the phases and constituents that were analyzed semi-quantitatively by energy-dispersive X-ray (EDX) microanalysis in the nitrated layers of Experiments 5 to 8. Table 6 shows the results thus obtained. It should be noted that pre-existing eutectic carbides of the  $\text{M}_7\text{C}_3$  type, transform into carbonitrides [32] after nitrating treatment (Spectra 1 and 3). The values show weight percentages exceeding 14 wt.%N. However, the matrix constituent of the nitrated layer reaches mean values of 4–8 wt.% N (Spectra 2,4,7,8,10 and 11) denoting lower N enrichment. Due to the low solubility of N in Fe and its higher affinity of this element for Cr and Mo (Ellingham diagram of nitride formation), it is reasonable to expect the presence of nitrides of Cr and Mo in tempered martensite, in addition to Fe–N system nitrides. This outmost layer is hard and yet very fragile. During the process of erosive wear peeling of this layer could occur, thus failing to provide further wear resistance. Spectra 5,6,9,12,13 and 14 show the approximate weight percentages of the elements that constitute the eutectic carbides  $\text{M}_7\text{C}_3$  and the eutectic constituent, formed by martensite, retained austenite and secondary carbides, which are located outside the nitride layer.



**Figure 4.** Representative image of the thickness of the nitrided layer. (a): Experiment 5; (b): Experiment 6; (c): Experiment 7; (d): Experiment 8.



**Figure 5.** Cont.

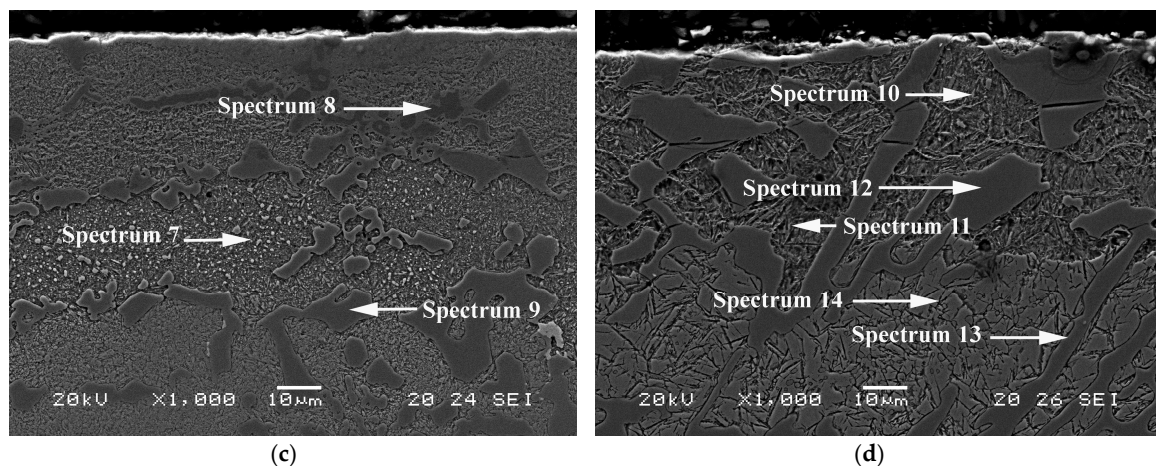


**Figure 5.** Phases and constituents in the nitrided layer analyzed by energy dispersive X-ray (EDX) microanalysis. (a) Experiment 5; (b) Experiment 6; (c) Experiment 7; (d) Experiment 8.

**Table 6.** Semi-quantitative analysis of the phases listed in Figure 5, determined by characteristic energy dispersive X-ray (EDX) microanalysis. (% in weight).

Figure	Exp.	Spectrum N	Si	Cr	Fe	Mo	Quenching			Tempering		
(a)	5	1	16.1	–	44.5	37.2	2.2	1000 °C	4 h	Oil	200 °C	3 h
		2	4.1	1.7	7.5	86.6	–					
		3	14.9	–	36.0	46.5	2.5					
(b)	6	4	8.4	1.7	10	77.3	2.6	1100 °C	4 h	Air	500 °C	3 h
		5	–	–	51.8	45.9	2.2					
		6	–	1.8	7.9	89.3	1.1					
(c)	7	7	15.1	–	48.3	34.7	1.8	1000 °C	8 h	Air	200 °C	6 h
		8	6.3	1.6	8.3	82.7	1.3					
		9	–	–	56.8	43.2	–					
(d)	8	10	6.7	2.3	8.9	80.7	1.4	1100 °C	8 h	Oil	500 °C	6 h
		11	8.6	2.2	8.9	78.6	1.7					
		12	15.2	–	42.4	39.3	3.1					
		13	–	–	51.8	45.5	2.6					
		14	–	1.8	8.1	89.5	0.7					

#### 4. Conclusions

With regard to hypoeutectic white cast irons with 18 wt.% Cr and 2 wt.% Mo, subjected to different heat treatments to destabilize austenite, different quench conditions, different tempering conditions, with or without ionic nitriding treatment, it is concluded that:

1. There is a difference between the Factors that condition the hardness of the material and those that condition its erosive wear resistance. The highest increase in hardness is obtained when the temperature employed to destabilize the austenite is 1000 °C and when the material is subjected to a nitriding treatment. However, the highest erosive wear resistance is obtained with the shortest dwell time at the destabilization temperature (4 h), quenching in oil, and employing the shortest tempering times (3 h).
2. Among the nitrided samples, it was found that the eutectic carbides located in the nitrided layer are transformed into carbonitrides and that the greater thicknesses of nitrided layers are obtained when the temperature employed to destabilize the austenite was 1000 °C and the tempering

temperature was 200 °C. However, despite what was expected, the nitriding treatment does not have a significant effect on erosive wear resistance.

**Author Contributions:** J.A.-L. conceived and designed the experiments; A.G.-P. performed the experiments; and F.A.-A. analyzed the data and wrote the paper.

**Acknowledgments:** To carry out this study, we are grateful to the Spanish company Acutrim, and in particular we thank the Director of the company, Joaquim Morell, for the help provided in the nitriding of the samples.

**Conflicts of Interest:** The authors declare no conflict of interest.

## References

1. Pero-Sanz, J.A. *Fundiciones Férrreas*; Dossat: Madrid, Spain, 1994; p. 154.
2. Fairhurst, W.; Rohrig, K. Abrasion resistant high chromium cast irons. *Foundry Trade J.* **1974**, *136*, 685–698.
3. Ju, J.; Fu, H.G.; Fu, D.M.; Wei, S.Z.; Sang, P.; Wu, Z.W.; Tang, K.Z.; Lei, Y.P. Effects of Cr and V additions on the microstructure and properties of high-vanadium wear-resistant alloy steel. *Ironmak. Steelmak.* **2018**, *45*, 176–186. [[CrossRef](#)]
4. Bedolla-Jacuinde, A.; Arias, L.; Hernandez, B. Kinetics of secondary carbides precipitation in a high-chromium white iron. *J. Mater. Eng. Perform.* **2003**, *12*, 371–382. [[CrossRef](#)]
5. Heino, V.; Kallio, M.; Valtonen, K.; Kuokkala, V.T. The role of microstructure in high stress abrasion of white cast irons. *Wear* **2017**, *388*, 119–125. [[CrossRef](#)]
6. Filipovic, M.M. Iron-chromium-carbon-vanadium white cast irons—The microstructure and properties. *Hem. Ind.* **2014**, *68*, 413–427. [[CrossRef](#)]
7. Guitar, M.A.; Suarez, S.; Prat, O.; Guigou, M.D.; Gari, V.; Pereira, G.; Mucklich, F. High Chromium Cast Irons: Destabilized-Subcritical Secondary Carbide Precipitation and Its Effect on Hardness and Wear Properties. *J. Mater. Eng. Perform.* **2018**, *27*, 3877–3885. [[CrossRef](#)]
8. Gasan, H.; Erturk, F. Effects of a Destabilization Heat Treatment on the Microstructure and Abrasive Wear Behavior of High-Chromium White Cast Iron Investigated Using Different Characterization Techniques. *Metall. Mater. Trans. A Phys. Metall. Mater. Sci.* **2013**, *44*, 4993–5005. [[CrossRef](#)]
9. Lai, J.P.; Pan, Q.L.; Sun, Y.W.; Xiao, C.A. Effect of Si Content on the Microstructure and Wear Resistance of High Chromium Cast Iron. *ISIJ Int.* **2018**, *58*, 1532–1537. [[CrossRef](#)]
10. Antolin, J.F.A.; Garrote, L.F.; Lozano, J.A. Application of Rietveld Refinement to the correlation of the microstructure evolution of white cast irons with 18 and 25 %-wt. Cr after oil quench and successive temper treatments, with abrasive wear and bending testing. *Rev. Metal.* **2018**, *54*, 11. [[CrossRef](#)]
11. Bedolla-Jacuinde, A.; Guerra, F.V.; Mejia, I.; Zuno-Silva, J.; Rainforth, M. Abrasive wear of V-Nb-Ti alloyed high-chromium white irons. *Wear* **2015**, *332*, 1006–1011. [[CrossRef](#)]
12. Efremenko, V.; Shimizu, K.; Chabak, Y. Effect of Destabilizing Heat Treatment on Solid-State Phase Transformation in High-Chromium Cast Irons. *Metall. Mater. Trans. A Phys. Metall. Mater. Sci.* **2013**, *44*, 5434–5446. [[CrossRef](#)]
13. Liu, Q.; Shibata, H.; Hedstrom, P.; Joonsson, P.G.; Nakajima, K. Dynamic Precipitation Behavior of Secondary M7C3 Carbides in Ti-alloyed High Chromium Cast Iron. *ISIJ Int.* **2013**, *53*, 1237–1244. [[CrossRef](#)]
14. Wiengmoon, A.; Pearce, J.T.H.; Chairuangsi, T. Relationship between microstructure, hardness and corrosion resistance in 20 wt.%Cr, 27 wt.%Cr and 36 wt.%Cr high chromium cast irons. *Mater. Chem. Phys.* **2011**, *125*, 739–748. [[CrossRef](#)]
15. Karantzalis, A.E.; Lekatou, A.; Diavati, E. Effect of Destabilization Heat Treatments on the Microstructure of High-Chromium Cast Iron: A Microscopy Examination Approach. *J. Mater. Eng. Perform.* **2009**, *18*, 1078–1085. [[CrossRef](#)]
16. Kootsookos, A.; Gates, J.D. The role of secondary carbide precipitation on the fracture toughness of a reduced carbon white iron. *Mater. Sci. Eng. A Struct. Mater. Prop. Microstruct. Process.* **2008**, *490*, 313–318. [[CrossRef](#)]
17. Carpenter, S.D.; Carpenter, D.; Pearce, J.T.H. XRD and electron microscope study of a heat treated 26.6% chromium white iron microstructure. *Mater. Chem. Phys.* **2007**, *101*, 49–55. [[CrossRef](#)]
18. Wang, J.; Sun, Z.P.; Zuo, R.L.; Li, C.; Shen, B.L.; Gao, S.J.; Huang, S.J. Effects of secondary carbide precipitation and transformation on abrasion resistance of the 16Cr-1Mo-1Cu white iron. *J. Mater. Eng. Perform.* **2006**, *15*, 316–319. [[CrossRef](#)]

19. Pearce, J.T.H. Structural characterisation of high chromium cast irons. In Proceedings of the International Conference on Solidification Science and Processing: Outlook for the 21st Century, Bangalore, India, 18–21 February 2001; pp. 241–247.
20. Wang, J.; Li, C.; Liu, H.H.; Yang, H.S.; Shen, B.L.; Gao, S.J.; Huang, S.J. The precipitation and transformation of secondary carbides in a high chromium cast iron. *Mater. Charact.* **2006**, *56*, 73–78. [[CrossRef](#)]
21. Fernandez-Pariente, I.; Belzunce-Varela, F.J. Influence of different heat treatments on the microstructure of a high chromium white cast iron. *Rev. Metal.* **2006**, *42*, 279–286. [[CrossRef](#)]
22. Tenorio, J.A.S.; Albertin, E.; Espinosa, D.C.R. Effects of Mo additions on the solidification of high chromium cast iron. *Int. J. Cast Met. Res.* **2000**, *13*, 99–105. [[CrossRef](#)]
23. Karantzalis, E.; Lekatou, A.; Mavros, H. Microstructure and properties of high chromium cast irons: Effect of heat treatments and alloying additions. *Int. J. Cast Met. Res.* **2009**, *22*, 448–456. [[CrossRef](#)]
24. Cetinkaya, C. An investigation of the wear behaviours of white cast irons under different compositions. *Mater. Des.* **2006**, *27*, 437–445. [[CrossRef](#)]
25. Li, Y.C.; Li, P.; Wang, K.; Li, H.Z.; Gong, M.Y.; Tong, W.P. Microstructure and mechanical properties of a Mo alloyed high chromium cast iron after different heat treatments. *Vacuum* **2018**, *156*, 59–67. [[CrossRef](#)]
26. Scandian, C.; Boher, C.; de Mello, J.D.B.; Rezai-Aria, F. Effect of molybdenum and chromium contents in sliding wear of high-chromium white cast iron: The relationship between microstructure and wear. *Wear* **2009**, *267*, 401–408. [[CrossRef](#)]
27. Oh, H.; Lee, S.; Jung, J.Y.; Ahn, S. Correlation of microstructure with the wear resistance and fracture toughness of duocast materials composed of high-chromium white cast iron and low-chromium steel. *Metall. Mater. Trans. A Phys. Metall. Mater. Sci.* **2001**, *32*, 515–524. [[CrossRef](#)]
28. Nurjaman, F.; Sumardi, S.; Shofi, A.; Aryati, M.; Suharno, B. Effect of Molybdenum, Vanadium, Boron on Mechanical Properties of High Chromium White Cast Iron in As-Cast Condition. In Proceedings of the International Symposium on Frontier of Applied Physics (ISFAP), Bandung, Indonesia, 5–7 October 2016.
29. Pero-Sanz, J.A. *Aceros*; Dossat: Madrid, Spain, 2004; p. 558.
30. Steiner, T.; Meka, S.R.; Bischoff, E.; Waldenmaier, T.; Mittemeijer, E.J. Nitriding of ternary Fe-Cr-Mo alloys; role of the Cr/Mo-ratio. *Surf. Coat. Technol.* **2016**, *291*, 21–33. [[CrossRef](#)]
31. Prat-Bartés, A.; Tort-Martorell, X.; Grima-Cintas, P.; Pozueta-Fernández, L.; Solé-Vidal, I. *Métodos Estadísticos*, 2nd ed.; Cataluña, U.P.d., Ed.; Trillas: Jardines del Bosque, Mexico, 2004; p. 376.
32. Tancret, F.; Laigo, J.; Christien, F.; Le Gall, R.; Furtado, J. Phase transformations in Fe-Ni-Cr heat-resistant alloys for reformer tube applications. *Mater. Sci. Technol.* **2018**, *34*, 1333–1343. [[CrossRef](#)]

